Using nine years of Swarm magnetic field observations to estimate ionospheric electric current density through the curl-B technique

INGV terremoti vulcani ambiente — ISTITUTO NAZIONALE DI GEOFISICA E VULCANOLOGIA

Roberta Tozzi*, Tommaso Alberti, Igino Coco, Paola De Michelis, Fabio Giannattasio, Michael Pezzopane, and Alessio Pignalberi

Istituto Nazionale di Geofisica e Vulcanologia

* roberta.tozzi@ingv.it

EGU23-15406

Introduction & Data Selection

One of the features that characterises the three-satellite Swarm constellation (launched in November 2013) relates to its geometrical configuration. Two satellites (Swarm A and C) orbit the Earth in tandem at the same altitude while the third (Swarm B) flies about 50 km above them.

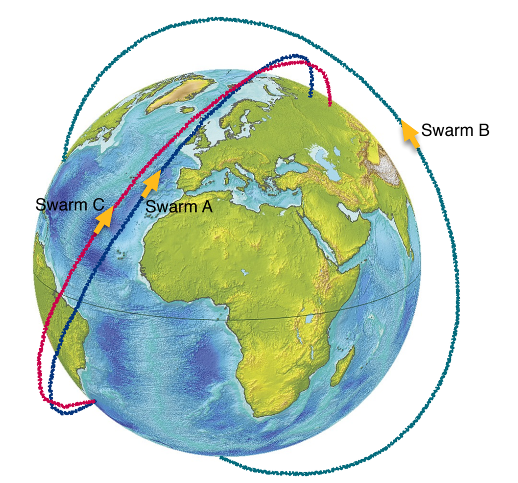

The availability of observations of the geomagnetic field on the surface of two spherical shells (i.e. those swept by Swam A/C and by Swarm B) allows estimating differential operators of the magnetic field Swarm satellites go through, directly from measured data without the need to model its variations in space in advance.

Electric currents (**J**) and related magnetic fields (**B**) are linked through the fourth Maxwell equation:

$$\mathbf{J} = \frac{1}{\mu_0} \nabla \times \mathbf{B}$$

with μ_0 magnetic permeability of free space.

In spherical coordinates this equation translates into:

$$J_r = \frac{1}{r sin\theta}\left(\frac{\partial}{\partial\theta} sin\theta B_\phi - \frac{\partial B_\theta}{\partial\phi}\right)$$
$$J_\theta = \frac{1}{r}\left(\frac{1}{sin\theta}\frac{\partial B_r}{\partial\phi} - \frac{\partial}{\partial r} r B_\phi\right) \qquad (1)$$
$$J_\phi = \frac{1}{r}\left(\frac{\partial}{\partial r} r B_\theta - \frac{\partial B_r}{\partial\theta}\right)$$

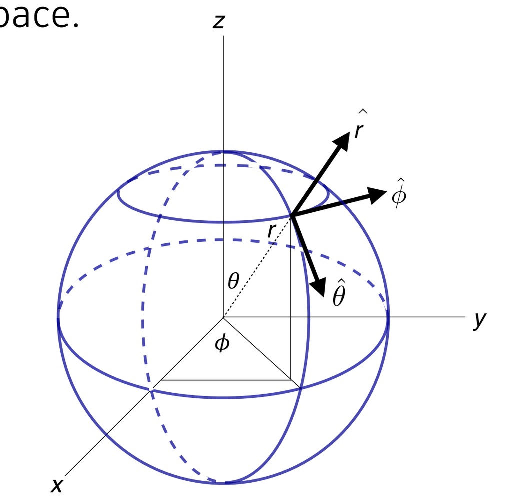

The above current densities, if calculated using the observed ionospheric component of the Earth's magnetic, provides the radial, meridional and zonal components of the ionospheric current density **J** at Swarm altitude (Tozzi et al., 2015, GRL).

Data used consist of low resolution (i.e. 1 Hz sampling) vector magnetic measurements collected on-board Swarm A and B from the 15th of March 2014 to the 6th of July 2022. Although even more recent Swarm data are available, the investigated time interval depends on the availability of geomagnetic activity indices used to calculate currents for two different levels of geomagnetic conditions (see below).

Main, crustal and magnetospheric Earth's magnetic field components have been modeled by means of CHAOS-7 and removed from observed data so to isolate the ionospheric component of the Earth's magnetic field from the other contributions.

Data have been then selected according to geomagnetic activity as described by the SuperMAG (Gjerloev, 2012, JGR) indices SMR and SME. These are representative of the dynamics at low-middle latitudes and high latitudes being a sort of equivalent of Sym-H and AE indices, respectively. So, quiet and disturbed conditions, have been defined as follows:

Quiet: -5 nT < SMR < 5 nT and SME < 50 nT
Disturbed: SMR < -25 nT and SME > 350 nT

Data Processing & Analysis

Data from each satellite are arranged, according to their coordinates (θ, ϕ) in 2°x 2° bins to cover the entire range of colatitudes and longitudes (90 bins in latitude and 180 in longitude).

Values of B_θ, B_ϕ and B_r falling in each bin for both Swarm A and B are averaged and matrices with elements $B_{\theta x}^{j,k}$, $B_{\phi x}^{j,k}$ and $B_{rx}^{j,k}$ (j=1,90, k=1,180 and x=A or B) are created (Figure 1B). Similarly, values of the radial distance from the Earth are transformed into two matrices with elements $R_A^{j,k}$ and $R_B^{j,k}$.
Being interested in large scales features of current density we applied a low-pass Gaussian filter with a cut-off frequency corresponding to scale lengths of about 3500 km (Figure 1C) to all the matrices.

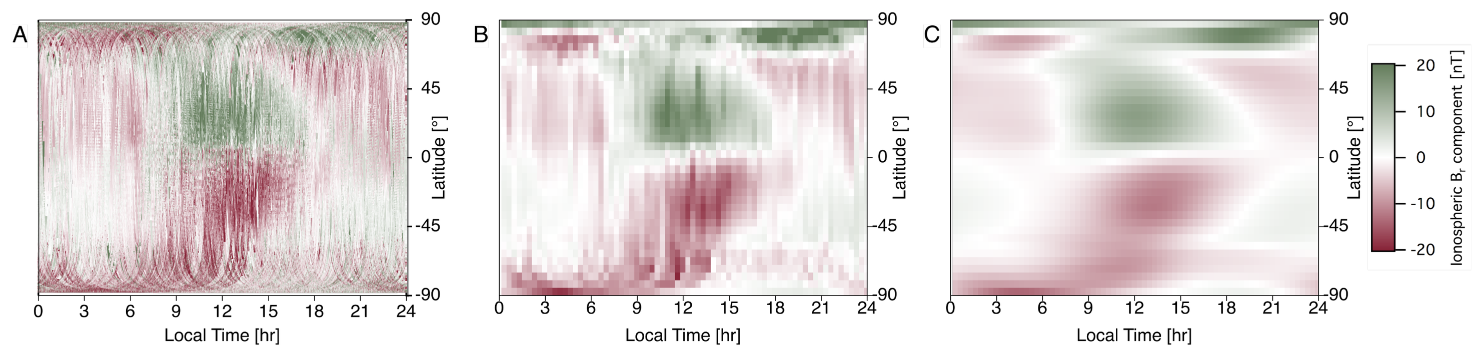

Fig. 1 Sequence of data processing steps applied to the radial component B_r of the ionospheric magnetic field derived from Swarm B. A) All data after selection for geomagnetically quiet conditions; B) Average values of data after arrangement into $B_{rB}^{j,k}$ matrix; C) same as B after low-pass Gaussian filter.

To estimate the components J_r, J_θ, and J_ϕ of the current density in the spherical frame, we used the following formulas that are the translation of equations (1) in terms of discrete observed data:

$$J_r^{j,k} = \frac{1}{\mu_0}\frac{1}{R_A^{j,k} sin\theta_j}\left[\frac{sin\theta_{j+1}B_{\phi A}^{j+1,k} - sin\theta_j B_{\phi A}^{j,k}}{\Delta\theta} - \frac{B_{\theta A}^{j,k+1} - B_{\theta A}^{j,k}}{\Delta\phi}\right]$$
$$J_\theta^{j,k} = \frac{1}{\mu_0}\frac{1}{R_A^{j,k}}\left[\frac{B_{rA}^{j,k+1} - B_{rA}^{j,k}}{sin\theta_j \Delta\phi} - \frac{R_B^{j,k}B_{\phi B}^{j,k} - R_A^{j,k}B_{\phi A}^{j,k}}{R_B^{j,k} - R_A^{j,k}}\right] \qquad (2)$$
$$J_\phi^{j,k} = \frac{1}{\mu_0}\frac{1}{R_A^{j,k}}\left[\frac{R_B^{j,k}B_{\theta B}^{j,k} - R_A^{j,k}B_{\theta A}^{j,k}}{R_B^{j,k} - R_A^{j,k}} - \frac{B_{rA}^{j+1,k} - B_{rA}^{j,k}}{\Delta\theta}\right]$$

Northern Hemisphere

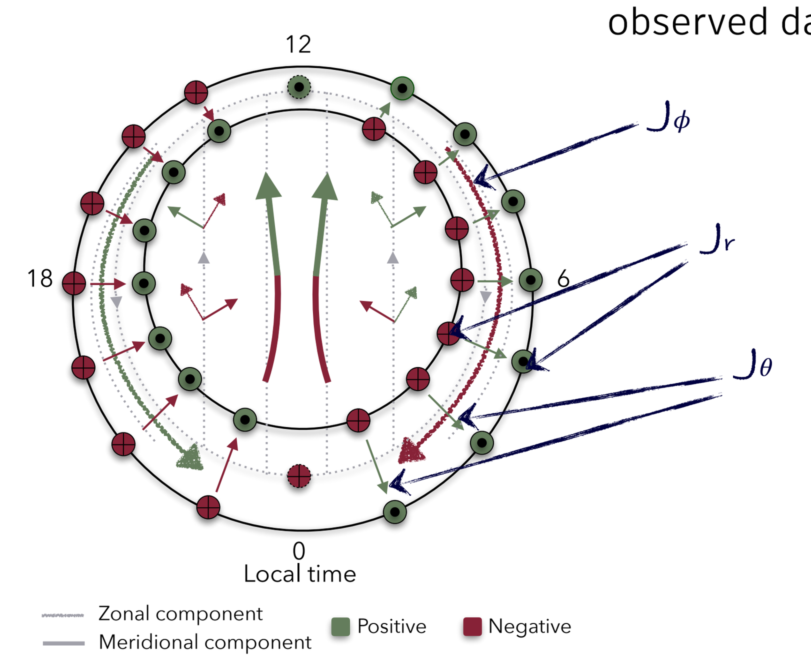

In this case, we used MLT in place of longitude; values of the matrices built according to equation (2) have been transformed into maps representing the climatological average (over the considered time interval) of the radial, meridional and zonal large scale current densities for quiet and disturbed geomagnetic conditions at ionospheric F-region altitudes.
Climatological maps obtained with almost 9 years of data are drawn for high latitudes (both polar regions, i.e. Figure 3) and middle and low latitudes (Figure 4).

Fig. 2 Sketch of horizontal and vertical polar currents as seen from above the Northern polar region. Signs are coherent with the geocentric frame: the <u>radial component is positive outward</u>, the <u>meridional component positive Southward</u> and the <u>zonal component is positive Eastward</u>.

Results

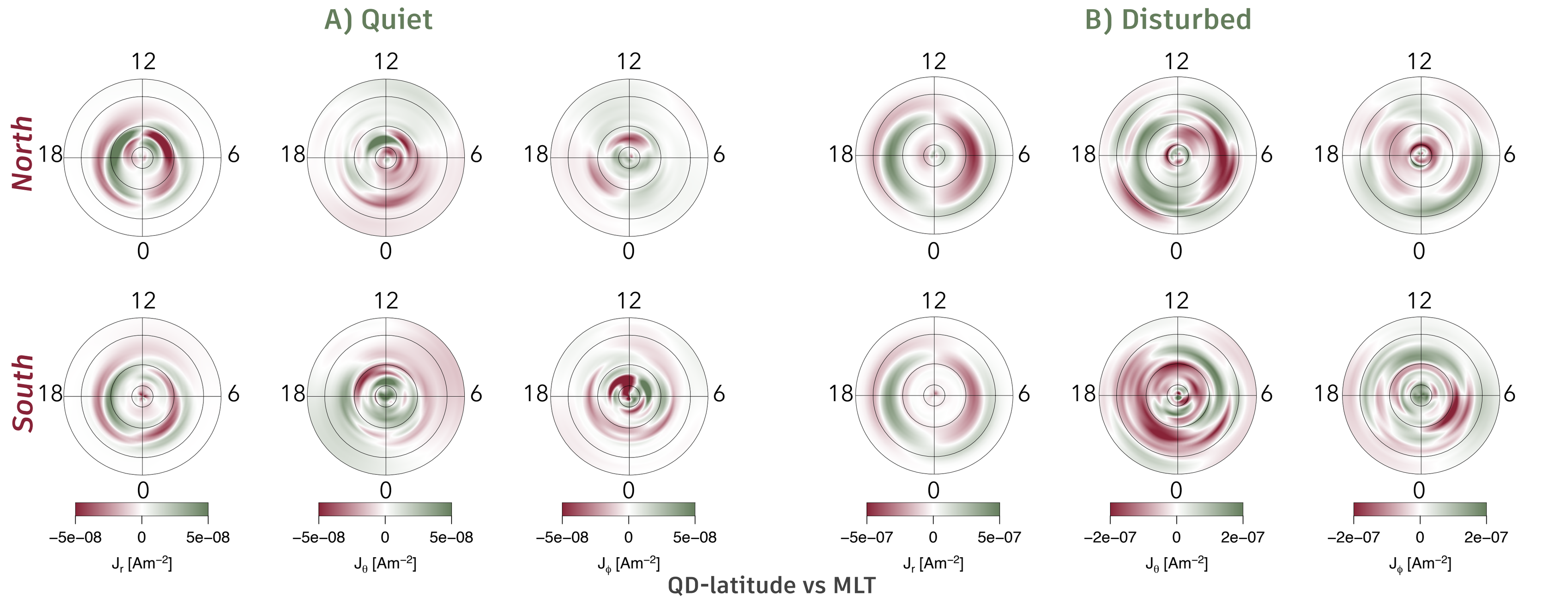

Fig. 3 Radial J_r (positive outward), meridional J_θ (positive Southward) and zonal J_ϕ (positive Eastward) components of the ionospheric electron density for the Northern (top row) and Southern (bottom row) polar regions, respectively, for quiet (A) and disturbed (B) conditions. Circles indicate 50°-60°-75°-85° QD-latitudes.

Figure 3 shows polar maps of electric current density components for quiet and disturbed conditions. The first column of Figures 3A and 3B show the curl-B reconstructed radial currents J_r. These currents well reproduce the features expected for the field aligned currents (FAC), i.e., morphology, location in latitude of Region 1 and Region 2 (both during quiet and disturbed conditions), order of magnitude of their intensity in terms of current density. At QD-latitudes around 85° it is possible to distinguish another structure inside R1, this is better visible in the Northern hemisphere and could be interpreted as the R0 current (Watanabe et al., 1998, JGR).

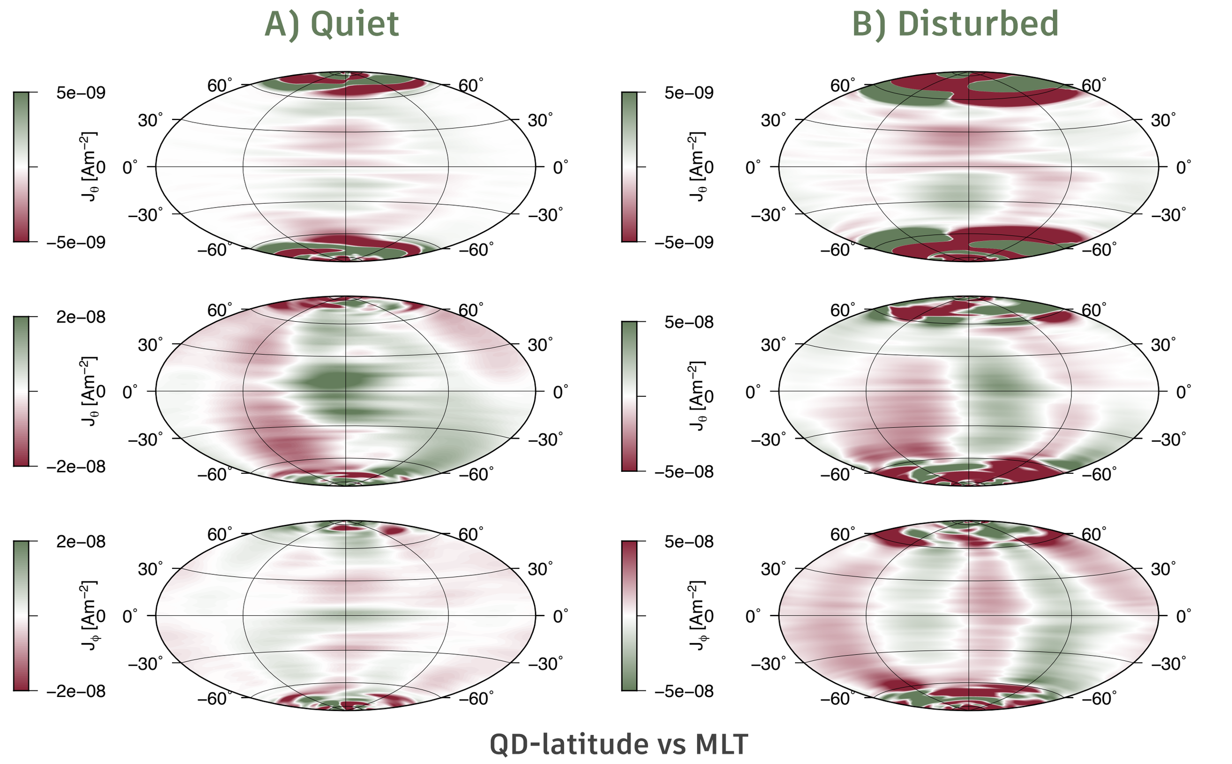

Fig. 4 Same as Figure 3 but for all latitudes. Maps centered at 12:00 MLT.

Figure 4 shows all-latitudes maps of J_r, J_θ and J_ϕ. Around noon, J_r displays features that agree, during both quiet and disturbed conditions, with those expected for the vertical component of the interhemispheric FACs (IHFAC). Top row of Figure 4 (A and B) shows the clear presence of a current flowing into the ionosphere, in the Northern hemisphere, and out of the ionosphere in the Southern hemisphere around noon.
Currents on the horizontal plane are much more difficult to interpret. Indeed, these currents include, for instance, the effects due to the F-region dynamo and the zonal electric fields and those due to the gravitational and pressure-gradient forces on the plasma (Maute and Richmond, 2017, SSR). A preliminary interpretation of the noon, equatorial portion of J_ϕ (quiet conditions) could be given in terms of the zonal current contributing to the closure of meridional (F region dynamo and return) current (Park et al., 2020, JGR). For a definitive understanding of the found J_θ and J_ϕ further analysis and investigations are needed.